J Opt (June 2017) 46(2):100–107
DOI 10.1007/s12596-016-0383-9

RESEARCH ARTICLE

Aspheric coefficients of deformation for a Cartesian oval surface

Juan Camilo Valencia-Estrada[1,2] · Marcelo Vaca Pereira-Ghirghi[2] · Zacarias Malacara-Hernández[2] · Héctor Alejandro Chaparro-Romo[2]

Received: 9 February 2016 / Accepted: 27 October 2016 / Published online: 26 November 2016

Abstract In this paper we propose a mathematical model as a theoretical and practical contribution to the theory of aspheric surfaces, that allows the geometrical calculation of an aspherical refractive surface in cylindrical coordinates (r, z), that correspond to a non-degenerated Cartesian oval of revolution, according to standard formulae [ISO-10110-12 (2007)], including: vertex curvature C, conical constant K and aspheric deformation coefficients A_4, A_6, A_8, A_{10} and A_{14}. The results are shown for an object and its respective image located at finite distances from the vertex (origin of coordinates) on the optical axis.

Keywords Aspheric lenses · Cartesian ovals · No-image optics · Spherical aberration free · Aspheric coefficients

Introduction

Cartesian ovals of revolution are refractive surfaces which form perfect images of an object point situated on the optical axis; that is to say, presenting refraction without introduction of spherical aberration. Cartesian ovals were described for the first time by Descartes [1], and have been studied by numerous authors Luneberg [2], Born and Wolf [3], Malacara-Hernández [4], and Wiston et al. [5] with an implicit mathematical representation.

They have been described as well by Hsueh et al. [6] using explicit trigonometrical representations, with recursive functions that are 4th degree solutions of the Fermat principle, by Valencia et al. [7], using explicit Cartesian representations, but with recurrent functions that are 4th degree solutions of the Fermat principle as well, and finite power series, up to the 8th degree, solving a non-linear differential equation that results from Snell law, by Gutierrez et al. [8], using explicit polar representations in some cases, and by Cho [9], using explicit representations with superconics.

This work aims to establish a better approximation of Cartesian ovals surfaces using the standard formulae according to ISO 10110-12 (2007) to describe an aspherical surface of revolution with aspherical coefficients of deformation up to the 14th degree. In order to achieve this aim, the coefficients established in [7], with 8th degree series, are included, adding up to the 14th degree.

The method used in this paper can be summarized: The coefficients to describe a good approximation to a Cartesian oval according to ISO 10110-12 (2007) are obtained using the results of [7]. These results are modified by means of the substitutions of the variables levered-distance $\pm\alpha f$ and focal-distance $\pm f$, for each case in [7], with the variables object-distance t_a and image-distance t_b, following the rules of signs of Descartes. With this procedure a singular series for all Cartesian ovals is obtained. The formulas for the coefficients are obtained equating the MacLaurin series approximation of the standard formula according to ISO 10110-12 (2007), with the singular series. Finally, results are checked using software with ray tracing.

✉ Marcelo Vaca Pereira-Ghirghi
rghirghi@hotmail.com

Juan Camilo Valencia-Estrada
camilo.valencia@oledcomm.com

[1] Oledcomm SAS, Université de Versailles Saint-Quentin-en-Yvelines, Cp. 78140 Vélizy-Villacoublay, France

[2] Optica, Centro de Investigaciones en Óptica A.C, Cp. 37150 León, Guanajuato, Mexico

Representation in power series

Cartesian ovals can be represented in Maclaurin series according to [7], with

$$z(r) = C_2\frac{r^2}{2f} + C_4\frac{r^4}{8f^3} + C_6\frac{2r^6}{32f^5} + C_8\frac{5r^8}{128f^7} + C_{10}\frac{4r^{10}}{1024f^9} + C_{12}\frac{28r^{12}}{4096f^{11}} + C_{14}\frac{24r^{14}}{16384f^{13}} + O(r^{16}) = \sum_{j=1}^{\infty} C_{2j}\frac{I_j r^{2j}}{(2f)^{2j-1}}, \quad (1)$$

with cylindrical abscissa r, cylindrical ordinate z , image distance f and coefficients C_2, which depend on the Cartesian ovals case according to [7]. Equation (1) can represent any rotationally symmetric refractive surface that does not introduce spherical aberration. Also, Eq. (1) is useful to represent all conical surfaces, which under certain circumstances have a refraction to perform a perfect image on the optical axis, of an object point situated on the same axis, i.e. a ellipsoid of revolution, when the object is at infinity, a hyperboloid of revolution when the image is at infinity, and a sphere when the object point and the image point are situated on its aplanatic points. Paraboloids of revolution when $C_2 = 1/2$ and $C_{2j} = 0$, for all $j \geq 2$, are not included, just because we are interested only in the reflective interfaces with perfect image.

Also, Eq. (1) can represent Cartesian ovals of revolution with meridional sections that not degenerate into a conic section, which form a perfect image of an object point situated on the same optical axis, both located at finite real or virtual distances from the vertex. According to reference [7], there are six fundamental cases of Cartesian ovals, defining two recurrent variables $m = n - 1$ and $p = n + 1$:

Case I: Natural oval with real object and real image

This oval without leverage (when the ratio between the absolute image distance and absolute object distance is equal to one) corresponds to a refractive interface with object distance $-f$ and image distance f, as is shown in Fig. 1a. It is assumed that the light departs from object space with a refractive index 1, to an image space with a relative refractive index n. In this case, coefficients C_{2j} are represented by Eq. (2).

$$\begin{aligned} C_2 &= \frac{p}{m}, \\ C_4 &= \frac{p}{m}, \\ C_6 &= \frac{p\,(n^2+6n+1)}{m^3}, \\ C_8 &= \frac{p}{m}, \\ C_{10} &= \frac{p\,(7n^4+124n^3+122n^2+124n+7)}{m^5}, \\ C_{12} &= \frac{p\,(3n^4-44n^3-46n^2-44n+3)}{m^5}, \\ C_{14} &= \frac{p\,(11n^6+534n^5+837n^4+1332n^3}{m^7} \\ &\quad + \frac{837n^2+534n+11)}{m^7}. \end{aligned} \quad (2)$$

Case II: Natural oval with virtual object and virtual image

This oval without leverage corresponds to a refractive interface with object distance f and image distance $-f$. In this case, coefficients C_{2j} are the same as in the previous case, but with opposite signs.

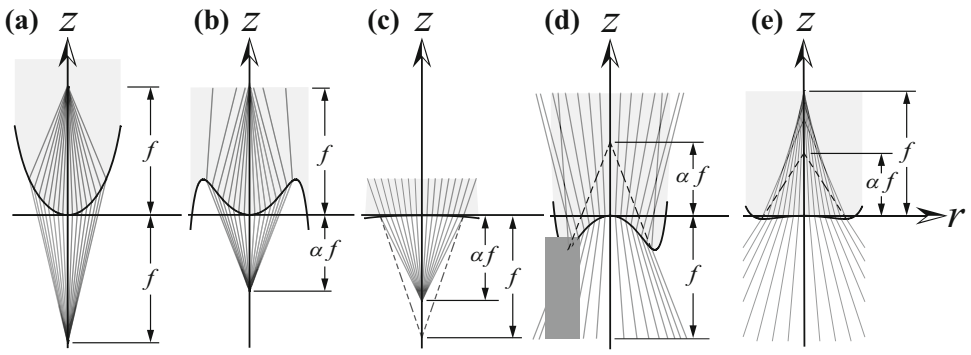

Fig. 1 Series approximations with five polynomial terms of several cases of Cartesian ovals. Upward ray tracing of five cases of Cartesian ovals, from a medium with a low refractive index to a medium with a high refractive index, according to [7], The following Figs. are shown: **a** Case I: Natural Cartesian oval with a real object and a real image. **b** Case III: Levered Cartesian oval with a real object and a real image. **c** Case IV: Levered Cartesian oval with a real object and a virtual image. **d** Case V: Levered Cartesian oval with a virtual object and a virtual image. **e** Case VI: Levered Cartesian oval with a virtual object an a real image

Case III: Leveraged oval with real object and real image

This corresponds to a refractive interface with object distance $-\alpha f$ and image distance f, with a leverage factor or proportion α, defined as positive (as our interest is not to form an image out of the axis, it is not appropriate to use a magnification in the place of a leverage) as is shown in Fig. 1b. In this case, coefficients C_2j are represented by Eq. (3) with the first sign, where it is possible to note that if leverage factor $\alpha = 1$, the coefficients according to Eq. (3) are reduced to the ones of Eq. (2).

Case IV: Leveraged oval with real object and virtual image

This corresponds to a refractive interface with object distance $-\alpha f$ and image distance $-f$, with a leverage factor or proportion α, defined as positive, as shown in Fig. 1c. In this case, coefficients C_{2j} are represented by Eq. (3) with the second sign, where we can note that if leverage factor $\alpha = 1$, coefficients according to Eq. (3) with the second sign are not reduced to any equation of previous coefficients.

$$
\left.
\begin{aligned}
C_2 &= \frac{\pm 1}{\alpha m}\,[\alpha n \pm 1],\\
C_4 &= \frac{\pm 1}{\alpha^3 m^2}\left[\alpha^3 n^2 + \left(\alpha^3 \pm 2\alpha^2 - 2\alpha \mp 1\right)n \mp 1\right],\\
C_6 &= \frac{\pm 1}{\alpha^5 m^3}\left[\begin{array}{c}\alpha^5 n^3 + \left(2\alpha^5 \pm 3\alpha^4 - 3\alpha^3 \pm \alpha^2 + 3\alpha \pm 1\right)n^2\\ +\left(\alpha^5 \pm 3\alpha^4 + \alpha^3 \mp 3\alpha^2 + 3\alpha \pm 2\right)n \pm 1\end{array}\right],\\
C_8 &= \frac{\pm 1}{\alpha^7 m^4}\left[\begin{array}{c}\alpha^7 n^4 + \left(3\alpha^7 \pm 4\alpha^6 - 4\alpha^5 \pm 2\alpha^4 + 2\alpha^3 \mp 4\alpha^2 - 4\alpha \mp 1\right)n^3 + \left(3\alpha^7 \pm 8\alpha^6 \mp 8\alpha^4\right.\\ \left.+8\alpha^3 - 8\alpha \mp 3\right)n^2 + \left(\alpha^7 \pm 4\alpha^6 + 4\alpha^5 \mp 2\alpha^4 - 2\alpha^3 \pm 4\alpha^2 - 4\alpha \mp 3\right)n \mp 1\end{array}\right],\\
C_{10} &= \frac{\pm 1}{\alpha^9 m^5}\left[\begin{array}{c}7\alpha^9 n^5 + \left(28\alpha^9 \pm 35\alpha^8 - 35\alpha^7 \pm 20\alpha^6 + 10\alpha^5 \mp 34\alpha^4 + 10\alpha^3 \pm 55\alpha^2 + 35\alpha \pm 7\right)n^4\\ +\left(42\alpha^9 \pm 105\alpha^8 - 15\alpha^7 \mp 90\alpha^6 + 126\alpha^5 \mp 30\alpha^4 - 100\alpha^3 \pm 75\alpha^2 + 105\alpha \pm 28\right)n^3\\ +\left(28\alpha^9 \pm 105\alpha^8 + 75\alpha^7 \mp 100\alpha^6 - 30\alpha^5 \pm 126\alpha^4 - 90\alpha^3 \mp 15\alpha^2 + 105\alpha \pm 42\right)n^2\\ +\left(7\alpha^9 \pm 35\alpha^8 + 55\alpha^7 \pm 10\alpha^6 - 34\alpha^5 \pm 10\alpha^4 + 20\alpha^3 \mp 35\alpha^2 + 35\alpha \pm 28\right)n \pm 7\end{array}\right],\\
C_{12} &= \frac{\pm 1}{\alpha^{11} m^6}\left[\begin{array}{c}3a^{11} n^6 + \left(15\alpha^{11} \pm 18\alpha^{10} - 18\alpha^9 \pm 11\alpha^8 + 3\alpha^7 \mp 16\alpha^6 + 12\alpha^5 \pm 15\alpha^4 - 25\alpha^3 \mp 38\alpha^2\right.\\ \left.-18\alpha \mp 3\right)n^5 + \left(30\alpha^{11} \pm 72\alpha^{10} - 16\alpha^9 \mp 54\alpha^8 + 90\alpha^7 \mp 44\alpha^6 - 60\alpha^5 \pm 90\alpha^4 + 26\alpha^3\right.\\ \left.\mp 96\alpha^2 - 72\alpha \mp 15\right)n^4 + \left(30\alpha^{11} \pm 108\alpha^{10} + 60\alpha^9 \mp 116\alpha^8 + 12\alpha^7 \pm 140\alpha^6 - 140\alpha^5\right.\\ \left.\mp 12\alpha^4 + 116\alpha^3 \mp 60\alpha^2 - 108\alpha \mp 30\right)n^3 + \left(15\alpha^{11} \pm 72\alpha^{10} + 96\alpha^9 \mp 26\alpha^8 - 90\alpha^7\right.\\ \left.\pm 60\alpha^6 + 44\alpha^5 \mp 90\alpha^4 + 54\alpha^3 \pm 16\alpha^2 - 72\alpha \mp 30\right)n^2 + \left(3\alpha^{11} \pm 18\alpha^{10} + 38\alpha^9 \pm 25\alpha^8\right.\\ \left.-15\alpha^7 \mp 12\alpha^6 + 16\alpha^5 \mp 3\alpha^4 - 11\alpha^3 \pm 18\alpha^2 - 18\alpha \mp 15\right)n \mp 3\end{array}\right],\\
C_{14} &= \frac{\pm 1}{\alpha^{13} m^7}\left[\begin{array}{c}11\alpha^{13} n^7 + \left(66\alpha^{13} \pm 77\alpha^{12} - 77\alpha^{11} \pm 49\alpha^{10} + 7\alpha^9 \mp 63\alpha^8 + 63\alpha^7 \pm 27\alpha^6\right.\\ \left.-119\alpha^5 \pm 7\alpha^4 + 217\alpha^3 \pm 203\alpha^2 + 77\alpha \pm 11\right)n^6 + \left(165\alpha^{13} \pm 385\alpha^{12} - 105\alpha^{11}\right.\\ \left.\mp 259\alpha^{10} + 483\alpha^9 \mp 315\alpha^8 - 225\alpha^7 \pm 595\alpha^6 - 147\alpha^5 \mp 637\alpha^4 + 245\alpha^3 \pm 735\alpha^2\right.\\ \left.+385\alpha \pm 66\right)n^5 + \left(220\alpha^{13} \pm 770\alpha^{12} + 350\alpha^{11} \mp 854\alpha^{10} + 294\alpha^9 \pm 882\alpha^8\right.\\ \left.-1330\alpha^7 \pm 230\alpha^6 + 1106\alpha^5 \mp 826\alpha^4 - 518\alpha^3 \pm 910\alpha^2 + 770\alpha \pm 165\right)n^4\\ +\left(165\alpha^{13} \pm 770\alpha^{12} + 910\alpha^{11} \mp 518\alpha^{10} - 826\alpha^9 \pm 1106\alpha^8 + 230\alpha^7 \mp 1330\alpha^6\right.\\ \left.+882\alpha^5 \pm 294\alpha^4 - 854\alpha^3 \pm 350\alpha^2 + 770\alpha \pm 220\right)n^3 + \left(66\alpha^{13} \pm 385\alpha^{12} + 735\alpha^{11}\right.\\ \left.\pm 245\alpha^{10} - 637\alpha^9 \mp 147\alpha^8 + 595\alpha^7 \mp 225\alpha^6 - 315\alpha^5 \pm 483\alpha^4 - 259\alpha^3\right.\\ \left.\mp 105\alpha^2 + 385\alpha \pm 165\right)n^2 + \left(11\alpha^{13} \mp 77\alpha^{12} + 203\alpha^{11} \pm 217\alpha^{10} + 7\alpha^9\right.\\ \left.\mp 119\alpha^8 + 27\alpha^7 \pm 63\alpha^6 - 63\alpha^5 \pm 7\alpha^4 - 49\alpha^3 \mp 77\alpha^2 + 77\alpha \pm 66\right)n \pm 11\end{array}\right].
\end{aligned}
\right\} \tag{3}
$$

Case V: Leveraged oval with virtual object and virtual image

This corresponds to a refractive interface with object distance αf and image distance $-f$, with leverage factor or proportion α, defined as positive, as is shown in Fig. 1c. In this case, coefficients $C_2 j$ are

$$\begin{aligned} C_2 &= -\frac{\alpha n+1}{\alpha m}, \\ C_4 &= -\frac{\alpha^3 n^2+(\alpha^3+2\alpha^2-2\alpha-1)n-1}{\alpha^3 m^2}, \\ &\vdots \end{aligned} \tag{4}$$

where we can note that with a leverage factor $\alpha = 1$, coefficients according to Eq. (4) are reduced to the case II coefficients, and they are the same coefficients of case III with opposite signs.

Case VI: Leveraged oval with virtual object and real image

This corresponds to a refractive interface with object distance αf and image distance f with a leverage factor or proportion α, defined as positive, as is shown in Fig. 1e. In this case, coefficients C_{2j} are

$$C_2 = \frac{\alpha n-1}{\alpha m}, \quad C_4 = \frac{\alpha^3 n^2+\left(\alpha^3-2\alpha^2-2\alpha+1\right)n+1}{\alpha^3 m^2}, \ldots, \tag{5}$$

where we can note that if leverage factor $\alpha = 1$, coefficients according to Eq. (5) do not reduce to any previous coefficients; however, we note that the coefficients according Eq. (5) are the same as in case IV, but with opposite signs.

To simplify the model, it is convenient to represent all the previous cases with a unique formula. To achieve this, we have to use Descartes's rule of signs, specifying the object distance t_a and the image distance t_b from the vertex, as is shown in Fig. 2. As the first two cases (I and II), which correspond to the natural ovals, are included as particular leveraged cases (III and V), with $\alpha = 1$ in Eqs. (3) and (4), it is only necessary to combine the leveraged cases. Combining leveraged cases III and V with $\alpha = -t_a/t_b$ in Eqs. (3) with the first sign and (4), and combining leveraged cases IV and VI with $\alpha = t_a/t_b$ in Eqs. (3) with the second sign and (5), we can obtain all the combined cases with coefficients

$$C_{2j} = \frac{\mathrm{sign}(t_b)}{m^j t_a^{2j-1}} P_{2j}, \tag{6}$$

with polynomials P_{2j}:

$$\left.\begin{aligned}
P_2 &= [n t_a - t_b], \\
P_4 &= \left[n^2 t_a^3 + t_b^3 + n(t_a+t_b)(t_a^2 - 3t_a t_b + t_b^2)\right], \\
P_6 &= \begin{bmatrix} n p^2 t_a^5 - 3n p\, t_a^4 t_b - n(3n-1) t_a^3 t_b^2 \\ -n(n-3) t_a^2 t_b^3 + 3n p\, t_a t_b^4 - p^2 t_b^5 \end{bmatrix}, \\
P_8 &= \begin{bmatrix} n p^3 t_a^7 - 4n p^2 t_a^6 t_b - 4n m p\, t_a^5 t_b^2 - 2n[n(n-4)-1] t_a^4 t_b^3 \\ +2n[n(n+4)-1] t_a^3 t_b^4 + 4n m p\, t_a^2 t_b^5 - 4n p^2 t_a t_b^6 + p^3 t_b^7 \end{bmatrix}, \\
P_{10} &= \begin{bmatrix} 7n p^4 t_a^9 - 35n p^3 t_a^8 t_b - 5n(7n-11) p^2 t_a^7 t_b^2 - 10n p(2n^2 - 11n + 1) t_a^6 t_b^3 \\ +2n(5n^3 + 63n^2 - 15n - 17) t_a^5 t_b^4 + 2n(17n^3 + 15n^2 - 63n - 5) t_a^4 t_b^5 \\ +10n p(n^2 - 11n + 2) t_a^3 t_b^6 - 5n(11n-7) p^2 t_a^2 t_b^7 + 35n p^3 t_a t_b^8 - 7p^4 t_b^9 \end{bmatrix}, \\
P_{12} &= \begin{bmatrix} 3n p^5 t_a^{11} - 18n p^4 t_a^{10} t_b - 2n(9n-19) p^3 t_a^9 t_b^2 - n(11n^2 - 76n + 25) p^2 t_a^8 t_b^3 \\ +3n m p(n^2 + 30n + 5) t_a^7 t_b^4 + 4n(4n^4 + 11n^3 - 35n^2 - 15n + 3) t_a^6 t_b^5 \\ +4n(3n^4 - 15n^3 - 35n^2 + 11n + 4) t_a^5 t_b^6 - 3n m p(5n^2 + 30n + 1) t_a^4 t_b^7 \\ -n(25n^2 - 76n + 11) p^2 t_a^3 t_b^8 + 2n(19n-9) p^3 t_a^2 t_b^9 - 18n p^4 t_a t_b^{10} + 3p^5 t_b^{11} \end{bmatrix}, \\
P_{14} &= \begin{bmatrix} 11n p^6 t_a^{13} - 77n p^5 t_a^{12} t_b - 7n(11n-29) p^4 t_a^{11} t_b^2 - 7n(7n^2 - 58n + 31) p^3 t_a^{10} t_b^3 \\ +7n(n^3 + 67n^2 - 93n + 1) p^2 t_a^9 t_b^4 + 7n(9n^4 + 36n^3 - 162n^2 + 4n + 17) p\, t_a^8 t_b^5 \\ +n(63n^5 - 225n^4 - 1330n^3 + 230n^2 + 595n + 27) t_a^7 t_b^6 - n(27n^5 + 595n^4 + 230n^3 \\ -1330n^2 - 225n + 63) t_a^6 t_b^7 - 7n p(17n^4 + 4n^3 - 162n^2 + 36n + 9) t_a^5 t_b^8 - 7n p^2 \\ (n^3 - 93n^2 + 67n + 1) t_a^4 t_b^9 + 7n p^3 (31n^2 - 58n + 7) t_a^3 t_b^{10} - 7n p^4 (29n-11) t_a^2 t_b^{11} \\ +77n p^5 t_a t_b^{12} - 11p^6 t_b^{13} \end{bmatrix}.
\end{aligned}\right\} \tag{7}$$

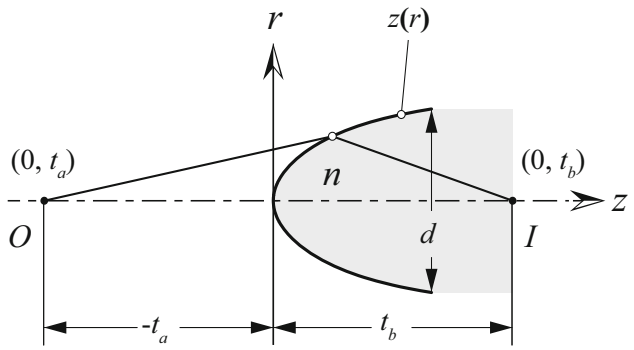

Fig. 2 Refraction in a Cartesian oval interface with real object O and real image I. One ray trace is shown from *left* to *right*

with recurrent variables $m = n - 1$ and $p = n + 1$.

The coefficients according to (6) should be replaced in the series Eq. (1) substituting $f \rightarrow |t_b| = \text{sign}(t_b)t_b$ to obtain

$$\begin{aligned} z(r) = \frac{1}{\text{sign}(t_b)}\Bigg(C_2\frac{r^2}{2t_b} + C_4\frac{r^4}{8t_b^3} + C_6\frac{r^6}{16t_b^5} \\ + C_8\frac{5r^8}{128t_b^7} + C_{10}\frac{r^{10}}{256t_b^9} + C_{12}\frac{7r^{12}}{1024t_b^{11}} \\ + C_{14}\frac{3r^{14}}{2048t_b^{13}} + O(r^{16})\Bigg) \\ = \sum_{j=1}^{\infty}\frac{C_{2j}}{\text{sign}(t_b)}\frac{I_j r^{2j}}{(2t_b)^{2j-1}}. \end{aligned} \tag{8}$$

The previous representation, Eq. (8) with coefficients according to Eq. (6), can be reduced to a singular series, valid for all Cartesian ovals:

$$\begin{aligned} z(r) = P_2\frac{r^2}{2mt_at_b} + P_4\frac{r^4}{8m^2t_a^3t_b^3} + P_6\frac{r^6}{16m^3t_a^5t_b^5} \\ + P_8\frac{5r^8}{128m^4t_a^7t_b^7} + P_{10}\frac{r^{10}}{256m^5t_a^9t_b^9} \\ + P_{12}\frac{7r^{12}}{1024m^6t_a^{11}t_b^{11}} + P_{14}\frac{3r^{14}}{2048m^7t_a^{13}t_b^{13}} \\ + O(r^{16}), = \sum_{j=1}^{\infty}\frac{P_{2j}I_j r^{2j}}{m^j(2t_at_b)^{2j-1}}, \end{aligned} \tag{9}$$

Representation following the standard ISO 10110-12 (2007)

Aspherical surfaces should be represented mathematically according with standard ISO 10110-12 (2007), using the formulae

$$z(r) = \frac{c\,r^2}{1 + \sqrt{1 - (1+K)(c\,r)^2}} + \sum_{j=2}^{\infty}A_{2j}r^{2j}, \tag{10}$$

where r is the cylindrical abscissa and z the respective ordinate, with prescribed parameters: vertex curvature c (which satisfies $c = 1/\rho$, whose ρ corresponds to the vertex curvature radius at the origin of coordinates), conical constant K, and the coefficients of deformation A_{2j} with respect to the conic of reference (base), for every integer $j \geq 2$. The representation Eq. (10) has the advantage that it can also represent flat surfaces and aspheric surfaces with null curvature at the vertex.

Some modern authors have suggested the name of "Schwarzschild's formula" for Eq. (10), however in [10] can clearly see that the original equation is shown in a non-rationalized form, and it does not allow to describe paraboloids of revolution surfaces or flat surfaces, and it does not include deformation coefficients. However the general equation for aspheric optics with deformation coefficients Eq. (10) dates back to 1932, when a Schmidts inner circle fellow found Bernhard Schmidt used an additional fourth degree coefficient to correct spherical aberration for his camera corrective plate. In said general equation, the deformation against a reference conical surface by using coefficients was proposed.

The original Schwarzschild representation can be obtained rationalizing the first summand in Eq. (10):

$$z(r) = \frac{1 - \sqrt{1 - (1+K)(c\,r)^2}}{c\,(1+K)} + \sum_{j=2}^{\infty}A_{2j}r^{2j}, \tag{11}$$

which does not allow the representation of aspherical surfaces with null curvature at the vertex, nor aspherical surfaces with parabolic meridional section with $K = -1$.

The surface Eq. (11) can also be represented using MacLaurin series; that is to say, expanding Eq. (11) in Taylor series around the vertex, with the fundamental formula:

$$z(r) = \sum_{k=1}^{\infty}Q_{2k}\,r^{2k} + \sum_{j=2}^{\infty}A_{2j}\,r^{2j}. \tag{12}$$

To determine coefficients Q_{2k}, we use the inverse $\mathbf{Z}$ transform ($\mathbf{Z}^{-1}$) of the function $z(r)$ to be expanded, evaluated in $r = 1/\mathbf{z}$, remembering that $\mathbf{z}$ is a dummy variable and is different from ordinate z:

$$Q_k = \mathbf{Z}^{-1}[z\,(1/\mathbf{z}), \mathbf{z}, k], \quad \forall\ \text{Int} \quad k = 1, 2, 3, \ldots, \infty. \tag{13}$$

Replacing the conical base of the representation Eq. (10) in Eq. (13), the $\mathbf{Z}^{-1}$ does not have analytical solution, but replacing the conical base of the conjugated representation Eq. (11), then it has an analytical representation with Eq. (14):

$$Q_k = \mathbf{Z}^{-1}\left[\frac{1-\sqrt{1-(1+K)\left(\frac{c}{\mathbf{z}}\right)^2}}{c(1+K)}, \mathbf{z}, k\right], \quad \forall \quad \text{Int}\, k = 1, 2, 3, \ldots, \infty,$$
$$= -\frac{[-c^2(1+K)]^{k/2}\,\text{Binomial}\left[\frac{1}{2}, \frac{k}{2}\right][1-\text{UnitStep}(-k)]\,\text{UnitStep}[-\text{Mod}(k,2)]}{c(1+K)}, \tag{14}$$

with non-null even coefficients for all k always even, because the aspherical base is rotationally symmetrical; that is, it is an even function, which means that Eq. (14) can be simplified with the substitution of $k = 2j$, for every positive integer j, removing all terms that involve unit step functions with a zero value, for all odd k values:

$$Q_{2j} = -\frac{[-c^2(1+K)]^j \text{Binomial}\left[\frac{1}{2}, j\right]}{c(1+K)}, \quad \forall \,\text{Int}\, j = 1, 2, 3, \ldots, \infty. \tag{15}$$

Substituting Eq. (15) in Eq. (12), we can obtain:

$$z(r) = \sum_{j=1}^{\infty}\left\{-\frac{[-c^2(1+K)]^j \text{Binomial}\left[\frac{1}{2}, j\right]}{c(1+K)}\, r^{2j}\right\} + \sum_{j=2}^{\infty} A_{2j}\, r^{2j}. \tag{16}$$

Combining representations

Matching coefficients of the representations in power series according to Eq. (9) with coefficients of the representation in power series Eq. (16) for each j, we can obtain a system of seven equations with eight unknowns:

$$\begin{aligned}
\frac{P_2}{2m\, t_a\, t_b} &= \frac{c}{2},\\
\frac{P_4}{8m^2\, t_a^3\, t_b^3} &= \frac{1}{8}c^3(1+K) + A_4,\\
\frac{P_6}{16m^3\, t_a^5\, t_b^5} &= \frac{1}{16}c^5(1+K)^2 + A_6,\\
\frac{5P_8}{128m^4\, t_a^7\, t_b^7} &= \frac{5}{128}c^7(1+K)^3 + A_8,\\
\frac{P_{10}}{256m^5\, t_a^9\, t_b^9} &= \frac{7}{256}c^9(1+K)^4 + A_{10},\\
\frac{7P_{12}}{1024m^6\, t_a^{11}\, t_b^{11}} &= \frac{21}{1024}c^{11}(1+K)^5 + A_{12},\\
\frac{3P_{14}}{2048m^7\, t_a^{13}\, t_b^{13}} &= \frac{33}{2048}c^{13}(1+K)^6 + A_{14},
\end{aligned} \tag{17}$$

with polynomials P_{2j} for $j = 1, 2, \ldots, 7$ according to Eq. (7). Solving for vertex curvature c in the first equation of Eq. (17)

$$c = \frac{1}{m}\left(\frac{n}{t_b} - \frac{1}{t_a}\right) = \frac{2U}{V}, \tag{18}$$

with recurrent variables $U = n\, t_a - t_b$ and $V = 2m\, t_a\, t_b$, which should be replaced in the following equations of Eq. (17) to ensure that these are not functions of the curvature. Solving all remaining equations of Eq. (17) for unknown deforming coefficients A_{2j}:

$$\begin{aligned}
A_4 &= \frac{mP_4 - U^3(1+K)}{V^3},\\
A_6 &= 2\left(\frac{m^2 P_6 - U^5(1+K)^2}{V^5}\right),\\
A_8 &= 5\left(\frac{m^3 P_8 - U^7(1+K)^3}{V^7}\right),\\
A_{10} &= 2\left(\frac{m^4 P_{10} - 7U^9(1+K)^4}{V^9}\right),\\
A_{12} &= 14\left(\frac{m^5 P_{12} - 3U^{11}(1+K)^5}{V^{11}}\right),\\
A_{14} &= 12\left(\frac{m^6 P_{14} - 11U^{13}(1+K)^6}{V^{13}}\right),
\end{aligned} \tag{19}$$

where we can note that there exist infinite solutions for A_{2j}, with a similar procedure according to [8], which will depend on the chosen conical constant. If we want to minimize the spherical aberration, there are several methods to choose the best conical constant; some are direct and others are indirect, and a lot of them require several numerical calculations. Here, we show a simple and indirect model to determine the best conical constant. This method guarantees that sagitta in the extreme of the field for a prescribed diameter, of both approximations defined by the series of Eqs. (9) or (10), match with sagitta of the rigorous solution, using the Fermat principle for all cases in the extreme of the field:

$$\begin{aligned}
-t_a + n\, t_b = &-\text{sign}(t_a)\sqrt{(d/2)^2 + (z(d/2) - t_a)^2}\\
&+ \text{sign}(t_b)\, n\sqrt{(d/2)^2 + (z(d/2) - t_b)^2},
\end{aligned} \tag{20}$$

where the solution for $z(d/2)$ can be obtained either analytically or numerically [6, 7] . With this sagitta at the edge of the field, we can determine the best conical constant which satisfies:

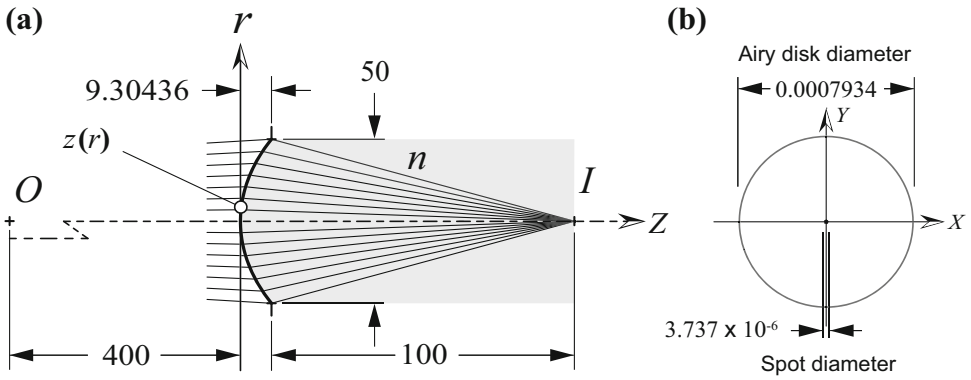

Fig. 3 Ray tracing of in a Cartesian oval interface with an ISO representation, with real object and real image using four deformation coefficients. The prescribed variables are: Object distance $t_a = -400$ (mm), image distance $t_b = 100$ (mm), relative refractive index $n = 1.7$ and the interface diameter $d = 50$ (mm). Calculated variables were: Entrance beam radius 24.4317 (mm), vertex curvature $c = 0.0278571$ (mm^{-1}), which is equivalent to a radius of curvature at the vertex of 35.89744 (mm), a conic constant $K = -0.471027$, and four deformation coefficients $A_4 = -1.06615 \times 10^{-7}$ (mm^{-3}), $A_6 = -1.22891 \times 10^{-11}$ (mm^{-5}), $A_8 = -2.25338 \times 10^{-15}$ (mm^{-7}) and $A_{10} = -3.57356 \times 10^{-19}$ (mm^{-9}). Figure3a shows a ray tracing with a diaphragm of a diameter d coupled to the surface. For the location of the diaphragm, the saggital solution $z(d/2) = 9.30436$ (mm) was found using Eq. (20). The calculation of the entrance beam radius was performed by similarity of triangles with $-t_a d/(2(z(d/2) - t_a))$. Figure3b shows the central spot with in Airy circle without performing any optimization neither defocus

$$z(d/2) = \sum_{j=1}^{\infty} \frac{P_{2j}\, I_j\, d^{2j}}{(n-1)^j\, 2^{2j}\, (2t_a\, t_b)^{2j-1}} = \left(\frac{c\, r^2}{1 + \sqrt{1 - (1+K)(c\, r)^2}} + \sum_{j=2}^{7} A_{2j}\, r^{2j} \right) |_{r=d/2}. \tag{21}$$

We can rewrite Eq. (21) as a polynomial of the unknown variable K. The polynomial degree will always be higher than four if one coefficient A_8, A_{10}, A_{12} or A_{14} is not zero; therefore, the ideal solution for K should be obtained numerically.

Results and conclusions

Using the same method used by Avendaño in [11], and Valencia et al. in [12], coefficients A_{2j} according to Eq. (19) can be verified analytically when the Cartesian oval degenerates into an ellipse, when the object distance $t_a \to \pm\infty$. Thus, the resulting coefficients Eq. (19) evaluated with $K = -1/n^2$ must vanish.

Also, the ISO formulas obtained were experimentally verified by running a computer program which allows one to obtain the best conic constant and deformation coefficients $A_4, A_6, A_8, A_{10}, A_{12}$ and A_{14}. After many checks, we conclude that six coefficients are not usually necessary because they have fast convergence for $F/\# > 1$, and only four are enough to get a small spot in most applications, unless extreme numerical aperture is required. Figure 3 shows one ray tracing done at OSLO®, with its respective central spot.

To determine when it is practical to use the approximate ISO formulas for a Cartesian oval, it is convenient to measure the result of ray tracing with a ratio of convergence that satisfies:

$$\Theta = \frac{\phi_{\text{Spot}}}{\phi_{\text{Airy disk}}} \leq 1 \tag{22}$$

Figure 4 shows a plot of points obtained with the information provided by OSLO® that results from ray tracing using four coefficients, for three indexes of refraction ($n = 1.5$, 1.7 and 1.9), with different diameters of the diaphragm coupled to the interface [$d = 10, 20, 30, 40$ and 50 (mm)] and different object distances ($t_a = -100$, $-200, -300$, and -400 (mm)), for one constant image distance $t_b = 100$ (mm), which allows determining when it is appropriate to use the deformation coefficients obtained for a prescribed $F/\#$.

It is clear from the results shown in Fig. 4 that the higher the refractive index, it is possible to obtain a lower ratio Θ at low $F/\#$. If the number of coefficients is increased to six, the results for $F/\# > 2$ do not differ much from those presented in Fig. 4. The maximum aperture of a Cartesian oval can be calculated with the solution for $d_{\max}$ of

$$\left.\frac{dz}{dr}\right|_{r=\frac{d_{\max}}{2}} = \frac{c\, d_{\max}}{\sqrt{4 - (1+K)(c\, d_{\max})^2}} + \sum_{j=2}^{\infty} 2jA_{2j}\, (d_{\max}/2)^{2j-1} = \frac{2\left(-t_a + z(d_{\max}/2)\right)}{d_{\max}}, \tag{23}$$

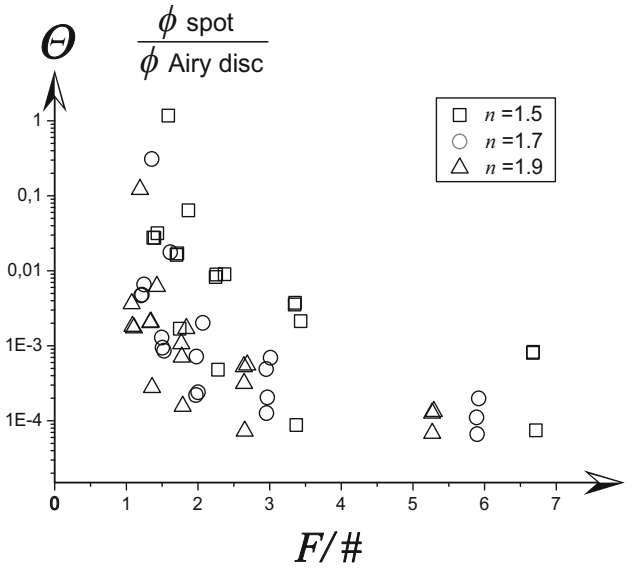

Fig. 4 Ratio of convergence of several ISO approximations of Catesian oval. Data $\{F/\#, \Theta\}$ were collected making calculations with the results of ray tracing in OSLO®, for three different refractive indexes according to combinations prescribed. It is observed that with higher refractive indices, the allowed $F/\#$ can be achieved with a very small ratio Θ, without optimization nor defocus, using only four deformation coefficients

when the slope of the Cartesian oval is equal to the slope of a tangent marginal ray. Eq. (23) applies when it has one real positive solution.

The coefficients obtained can be transformed to other representations (non-ISO) like Forbes's representation, [13]. In the early twentieth century, mass production of rotationally symmetric aspheric optical surfaces began to improve image quality in optical instruments. Then in the 40s, optical industry began to mass produce rotationally symmetrical aspheric surfaces, for use in optical instruments. In the 70s, production of Cartesian oval lenses for use in optical instruments and non-image optical systems began. Thus, we consider it is an appropriate time to incorporate these new technologies [14], which are developed to improve the quality of the optical systems.

Acknowledgements To the Centro de Investigaciones en Optica A.C. CIO, León, Guanajuato, México, and the Consejo Nacional de Ciencia y Tecnología de México, CONACyT, for its economic support.

Authors contribution JCVE developed most of the physical-mathematical model and programming. MVPG developed all simulations using OSLO®. ZMH developed the remained portion of the model and reviewed and verifed all results. ACR reviewed all equations and LaTeX edition. All authors gave final approval for publication.

Funding We currently have no funding or grants from anyone.

Compliance with ethical standards

Conflict of interest We have no competing interests.

Ethics statement This work did not involve any activity collection of human data, neither computer simulation of human behavior.

Data accessibility statement This work does not have any experimental data.

References

1. R. Descartes, *Discours de la méthode pour bien conduire sa raison et chercher la vérité dans les sciences, with three appendices: La Dioptrique* (Leyden, Leiden, 1637). https://fr.wikisource.org/wiki/Livre:Descartes_-_Discours_de_la_méthode,_éd._1637.djvu
2. R.K. Luneberg, *Mathematical Theory of Optics*, 1st edn. (University of California Press, Berkeley, 1964), pp. 139–151. (Section 24: Final Correction of Optical Instruments by Aspheric Surfaces)
3. M. Born, E. Wolf, *Principles of Optics*, 6th edn. (Pergamon Press, Oxford, 1980)
4. D. Malacara-Hernández, Z. Malacara-Hernández, *Handbook of Optical Design*, 2nd edn. (Marcel Dekker Inc., New York, 2004). (section 3.5, Equation (3.37))
5. R. Winston, J.C. Miñano, P. Benitez, *Nonimaging Optics* (Elsevier Academic Press, New York, 2005). ISBN: 0-12-759751-4
6. C. Hsueh, T. Elazhary, M. Nakano, J. Sasian, Closed-form sag solutions for Cartesian oval surfaces. J. Opt. **40**(4), 168–175 (2011)
7. J.C. Valencia-Estrada, A.H. Bedoya-Calle, D. Malacara-Hernández, Explicit representations of all refractive optical interfaces without spherical aberration. J. Opt. Soc. Am. A **30**, 1814–1824 (2013). doi:10.1364/JOSAA.30.001814
8. C.E. Gutierrez, Q. Huang, The near field refractor. Annales de l'Institut Henri Poincare (C) Non Linear Analysis, vol **31**, 4, pp 655–684 (2014)
9. S. Cho, Explicit Superconics Curves. J. Opt. Soc. Am. A **33**, 1822–1830 (2016). doi:10.1364/JOSAA.33.001822
10. K. Schwarzschild, Untersuchungen zur geometrischen Optik. II: Theorie der Spiegeltelescope (from Astronomische Mittheilungen der Koeniglichen Sternwarte zu Goettingen 1905). SPIE MILESTONE SERIES MS **73**, 3–3 (1993)
11. M. Avendaño-Alejo, Analytic formulas of the aspheric terms for convex-plano and plano-convex aspheric lenses. In Proc. SPIE 8841, Current Developments in Lens Design and Optical Engineering XIV, 88410E. Bellingham, WA:SPIE (2013). Doi:10.1117/12.2026366
12. J.C. Valencia-Estrada, R.B. Flores-Hernández, D. Malacara-Hernández, Singlet lenses free of all orders of spherical aberration. Proc. R. Soc. Lond. A Math. Phys. Eng. Sci. **471**, 2175 (2015)
13. G.W. Forbes, Shape specification for axially symmetric optical surfaces. Opt. Express **15**, 5218–5226 (2007). doi:10.1364/OE.15.005218
14. S. Kiontke, M. Demmler, M. Zeuner, F. Allenstein, T. Dunger, M. Nestler, Ion-beam figuring (IBF) for high-precision optics becomes affordable. In Proc. SPIE 7786, Current Developments in Lens Design and Optical Engineering XI; and Advances in Thin Film Coatings VI, 77860F (2010). Doi:10.1117/12.859127